Target selection signals causally influence human perceptual decision making

Daniel J. Pearce[1,†], Gerard M. Loughnane[2,†], Trevor T.-J. Chong[1], Nele Demeyere[3], Jason B. Mattingley[4,5], Margaret J. Moore[3,4], Peter W. New[6,7,8], Redmond G. O'Connell[1,2], Megan H. O'Neill[1], Dragan Rangelov[4,9], Renerus J. Stolwyk[1,10], Sam S. Webb[11], Shou-Han Zhou[12], Méadhbh B. Brosnan[1,11,13,14,15,*], and Mark A. Bellgrove[1,*]

[†]These authors contributed equally to this work.

[*]These authors contributed equally to this work.

Author affiliations:

1 School of Psychological Sciences and Turner Institute for Brain and Mental Health and, Monash University, Melbourne, VIC, 3800, Australia

2 National College of Ireland, Dublin 1, D01 K6W2, Ireland

3 Nuffield Department of Clinical Neurosciences, University of Oxford, Oxford, OX1 2JD, UK

4 Queensland Brain Institute, University of Queensland, Brisbane, QLD, 4072, Australia

5 School of Psychology, The University of Queensland, QLD, 4072, Australia

6 Aged and Rehabilitation Division, Medical Program, Monash Health, Melbourne, VIC, 3192, Australia

7 Epworth-Monash Rehabilitation Medicine Unit, Southern Medical School, VIC, 3121, Australia

8 Department of Epidemiology and Preventive Medicine, Monash University, VIC, 3800, Australia

9 School of Economics, The University of Queensland, QLD, 4072, Australia

10 Monash-Epworth Rehabilitation Research Centre, Melbourne, VIC, 3121, Australia

11 Department of Experimental Psychology, University of Oxford, Oxford, OX1 2JD, UK

12 Department of Psychology, James Cook University, QLD, 4811, Australia

13 Oxford Centre for Human Brain Activity, University of Oxford, Oxford, OX1 2JD, UK

14 Wellcome Centre for Integrative Neuroimaging, University of Oxford, Oxford, OX1 2JD, UK

15 School of Psychology, University College Dublin, Dublin 4, D04 C1P1, Ireland

Correspondence to: Daniel Pearce & Mark Bellgrove

Bellgrove Lab, Level 5, School of Psychological Sciences, Monash University, Melbourne, VIC, 3800, Australia

Daniel.Pearce1@monash.edu, Mark.Bellgrove@monash.edu

Running title: Target selection deficits impairs perceptual decision-making after stroke

Number of pages – 36. Number of figures – 4. Abstract, Introduction, Discussion.

Keywords: EEG; perception; decision-making; stroke; reaction time; attention.

Abstract

The ability to form decisions is a foundational cognitive function which is impaired across many psychiatric and neurological conditions. Understanding the neural processes underpinning clinical deficits may provide insights into the fundamental mechanisms of decision making. The N2c has been identified as an EEG signal indexing the efficiency of early target selection, which subsequently influences the timing of perceptual reports through modulating neural evidence accumulation rates. Evidence for the contribution of the N2c to human decision making however has thus far come from correlational research in neurologically healthy individuals. Here, we capitalised on the superior temporal resolution of EEG to show that unilateral brain lesions in male and female humans were associated with specific deficits in both the timing and strength of the N2c in the damaged hemisphere, with corresponding deficits in the timing of perceptual reports contralaterally. The extent to which the N2c influenced clinical deficits in perceptual reporting speed depended on neural rates of evidence accumulation. This work provides causal evidence that the N2c indexes an early, hemisphere-specific process supporting human decision making. This non-invasive EEG

marker could be used to monitor novel approaches for remediating clinical deficits in perceptual decision making across a range of brain disorders.

Significance Statement

Understanding how particular brain processes contribute to decision-making is crucial for our treatment of psychiatric and neurological disorders. This study provides causal evidence linking deficits in speed of visual processing to specific well-delineated EEG signals representing early target selection and evidence accumulation, in individuals with brain lesions. By showing how these lesions disrupt perceptual decisions, this work identifies a potential biomarker for decision-making deficits. This EEG measure offers a promising, non-invasive tool to track and refine treatments aimed at restoring decision-making abilities in affected patients.

Introduction

The speed at which individuals can make simple perceptual decisions is a foundational aspect of cognition which is negatively impacted by a wide range of neurological and psychiatric disorders (e.g. see Huang et al., 2015; Fosco et al., 2017; Fish et al., 2018). Understanding the neural processes underpinning these clinical deficits can provide insights into the fundamental mechanisms of perceptual decision making, aided by advances in human electroencephalography (EEG). A substantial body of research has demonstrated that a slow-building centro-parietal positivity EEG signal (the 'CPP') tracks the accumulation of sensory evidence and the formation of a decision across a wide range of tasks with varying sensory, perceptual, and higher cognitive requirements (Donner et al., 2009; De Lange et al., 2010; Wyart et al., 2012; Philiastides et al., 2014; Murphy et al., 2015; Loughnane et al., 2016; Spitzer et al., 2017; Afacan-Seref et al., 2018; Rungratsameetaweemana et al., 2018; Steinemann et al., 2018a; Herding et al., 2019; Tagliabue et al., 2019; van Vugt et al., 2019a; von Lautz et al., 2019). This signal bears remarkable similarities to evidence accumulation signals observed invasively in non-human primates (Kim and Shadlen, 1999; Shadlen and Newsome, 2001; Ding and Gold, 2012; Heitz and Schall, 2012; Mante et al., 2013).

Temporally preceding the evidence accumulation process is an earlier, hemisphere-specific posterior negativity, labelled the N2c, which indexes the selection of contralateral sensory targets from the environment (Loughnane et al., 2016; Newman et al., 2017; Brosnan et al., 2020). The N2c bears some similarity to the the family of EEG event-related potentials (ERPs) referred to as the N2 /N2pc (Luck and Hillyard, 1994; Eimer, 1996, 2014; Woodman and Luck, 1999; Kappenman and Luck, 2011) which are typically elicited using a target detection task and calculated as a subtraction waveform between trial conditions (Kappenman and Luck, 2011). The N2pc signal has been shown to relate to both distractor suppression (Luck and Hillyard, 1994; Luck, 2012), and target enhancement (Kiss et al., 2008; Hickey et al., 2009; Mazza et al., 2009). Using a task design that eliminated the typical Visual Evoked Potentials which appear in response to sudden-onset stimuli, Loughnane et al. (2016) isolated the specific aspect of the N2 related to target enhancement, contralateral to the target. The contralateral N2c predicted the timing of perceptual reports via both the onset and build-up rates of neural evidence accumulation (i.e. dynamics of the CPP; see also Nunez et al., 2019; Ghaderi-Kangavari et al., 2023).

A crucial aspect in identifying the relative importance of these EEG components along the sensorimotor transformation is to show whether they contribute to behaviour in a causal manner (O'Connell and Kelly, 2021). In non-human primates, several studies have used invasive methods such as inactivation and microstimulation to show the causal importance of certain neural populations to perceptual decision making (Hanks et al., 2006; Fleming et al., 2015; Katz et al., 2016; Yartsev et al., 2018; Derosiere et al., 2019; Zhou and Freedman, 2019). To date however, no such causal contribution has been investigated in humans with respect to the N2 component on behaviour. Yet this is important if we are to establish *bona fide* neural signals that might help to understand decision-making deficits in clinical disorders.

Here, we used a stroke patient lesion model to investigate the potential causal link between the N2 component and the timing of perceptual reports. A reliable phenomena following unilateral stroke damage is slowed responses to sensory stimuli presented to contralesional space, independently of response modality (Ballard et al., 2003; Johansson and Rönnbäck, 2012; Hurford et al., 2013). Using a bilateral variant of the random dot motion task (Kelly and O'Connell, 2013; Loughnane et al., 2016; Newman et al., 2017; Brosnan et al., 2020) we

looked at whether contralesional slowing of response time (RT) in stroke patients would be related to a disruption in the dynamics of early target selection signals.

Materials and methods

Participants

This research was approved by the Oxford Central University (MSD IDREC reference R61968/RE001), Monash Health (MHREC reference #14408A) and Monash University Human Research Ethics Committees (MUHREC reference #2492). All participants volunteered without knowledge of the hypotheses and provided written informed consent.

Neurologically Healthy Controls

Thirty-one (31) neurologically healthy adults (57-90 years, hereafter 'controls') were recruited from the community in Melbourne, Australia, of which 27 (13 males, 14 females) were included in the study (see Text S1 for details). Participants reported normal or corrected-to-normal visual acuity, self-reported being right-handed, were not taking arousal-modulating medications (such as tranquilisers) and reported no prior history of neurological or psychiatric conditions. All controls scored higher than 23/30 on the Montreal Cognitive Assessment (MoCA; Nasreddine et al., 2005) after adjusting for education.

Post-Stroke Adults

Seventy-one (71) individuals who had experienced a focal, first-ever clinically significant unilateral cerebral stroke (hereafter 'patients') were recruited from Melbourne, Australia and Oxford, UK. Of these, N=41 patients were excluded (n=16 did not successfully complete the task, n=21 had past history of neurological disorder on medical record review, and n=4 were removed due to data collection issues), leaving 30 patients (16 males, 14 females) for analysis (see Text S1 for more details). Patients were right-handed prior to their stroke, had a medically confirmed diagnosis of stroke, had no prior neurological or psychiatric history, reported normal or corrected-to-normal visual acuity, and had no reported use of arousal-altering medications. Participants did not have inferior visual field defects (i.e., where the visual stimuli were presented), as measured by a simple assessment (within the Oxford Cognitive Screen; OCS (Demeyere et al., 2015)) and did not have a primary extinction syndrome on a computerised

extinction task (Bender, 2011). Of these, *n*=2 participants used a left-hand response due to right-sided hemiplegia, and *n*=3 had upper quadrant visual field defects. See Tables 1 and 2 for participant demographics and stroke characteristics, respectively.

Procedure & Materials

All participants completed the Bilateral Random Dot Motion (BRDM) task (Loughnane et al., 2016; Brosnan et al., 2023; Fig. 1) while EEG was recorded. Eye movements were monitored with an EyeLink 1000 remote infrared eye-tracker (SR Research Ltd). To ensure that all patients and controls were fixating centrally (and not moving their eyes toward stimuli in either hemifield), pupils were monitored in real-time and if fixation was broken the trial ended and restarted once fixation was reestablished. The task was controlled via a Windows PC using MATLAB (MathWorks) and the Psychophysics Toolbox extensions (Brainard, 1997; Pelli, 1997; Cornelissen et al., 2002), and stimuli were displayed on either a 21-inch CRT monitor (Melbourne), or on a 23- or 27-inch LED monitor (Oxford). All monitors were set to a refresh rate of 85Hz and a screen resolution of 1024 x 768. Participants viewed the task from 57cm in a darkened, sound-attenuated room, with their head supported by a chin rest. Prior to completion of the BRDM EEG task, stroke patients completed a larger battery of cognitive tasks (Table 3), which are summarised in Text S1.

Assessment of Perceptual Decision-Making

The BRDM task (Newsome et al., 1989; Loughnane et al., 2016) is a computerised task that allows examination of how quickly and accurately responses are made separately for targets in each visual hemifield. Participants maintained central fixation while monitoring two peripheral circular patches that were positioned 10° either side and 4° below the fixation square, covering 8° visual angle (see Fig. 1). These patches consisted of 150 9x9 pixel randomly moving dots which were displaced by five degrees per second. At intervals of 1.8s, 2.8s, or 3.8s, 90% of the dots in either patch transitioned to moving uniformly either upward or downward. These target events occurred with equal probability in the left and right patches. Participants responded via a speeded single mouse click with their index finger upon detection of coherent motion targets. Trials restarted if a blink or gaze deviation more than four degrees left or right of centre was detected. Coherent motion pulses persisted for 3s or until a response was made.

Practice trials were administered until the participant understood the task, irrespective of their accuracy. Participants then completed 7 – 15 blocks of 24 trials. There were 12 possible trial types which varied according to the inter-stimulus interval (1.8s, 2.8s, or 3.8s), hemifield of target (left or right), and motion direction (up or down), with each presented twice per block in pseudorandom order. Rest breaks up to 180 seconds followed each block.

Electroencephalography (EEG)

Continuous EEG were acquired from either 64 scalp electrodes using a BrainAmp DC system (Brain Products), digitised at 500Hz (Melbourne), or 64 electrodes using a Neuroscan SynAmpsRT system, digitised at 1000Hz (Oxford), while participants completed the BRDM. We used a combination of custom scripts (available at https://osf.io/mvehu/?view_only=12aef65f46e246fcb94b1e8bd6dba040) and EEGLAB routines (Delorme and Makeig, 2004) implemented in MATLAB (MathWorks) to process the data.

Pre-Processing

First, we manually inspected channel variances for artifacts. We then accounted for cross-site differences in data collection by re-aligning the channels according to a common subset of 58 electrodes, and re-sampling Oxford data from 1000 to 500 Hz. Thereafter, all data were treated consistently. Data were detrended and we eliminated line noise by applying notch filters at 50, 100, and 150 Hz. We then applied a 0.1 Hz Hamming windowed sinc FIR high-pass filter. Channels previously identified as demonstrating zero or extreme variance were interpolated via spherical spline (mean channels interpolated = 1.95, median = 0). The interpolated data were then low-pass filtered at 8 Hz (120 Hz for spectral analyses), and re-referenced to the average.

A trial was defined as the period between central fixation and either a response, a fixation break, or onset of new random motion stimulus, as identified using EEG-recorded triggers. We extracted epochs from -200ms pre-target onset to 3000ms post-target onset (i.e., target offset), while response-locked epochs were extracted from -500ms pre-response to 100ms post-response. We then removed trials meeting any of the following conditions: (1) one or more EEG channels exceeded 100 μV between baseline (200 ms pre-target onset) and 100ms post-response, or between baseline and 1000 ms post-target onset; or (2) the participant blinked or

deviated their gaze by more than 3° left or right of centre during the same time window. Finally, we applied a Current Source Density transformation with a spline flexibility of 4 to disentangle overlapping ERP components (Kayser and Tenke, 2006), and baselined the stimulus- and response-locked ERP waveforms relative to -200 to 0 ms pre-stimulus onset.

Event-Related Potential (ERP) Extraction

CPP and N2 waveforms were derived by aggregating the baseline-corrected epochs at relevant electrodes separately for left and right hemifield targets. Consistent with our previous publications (Loughnane et al., 2016; Newman et al., 2017; Brosnan et al., 2020, 2023), we extracted the N2c contralateral to target location at peak electrodes P8 and P7 for left and right hemifield targets, respectively. The ipsilateral N2i component was extracted at peak electrodes P8/TP8 and P7/TP7. The CPP was measured centrally at peak electrode Pz irrespective of target hemifield (O'Connell et al., 2012; Kelly and O'Connell, 2013; Twomey et al., 2015; Loughnane et al., 2016; Newman et al., 2017; Brosnan et al., 2023).

We subsequently derived several metrics for each of the stimulus-locked ERP waveforms on a single-trial basis for each participant. The peak latency of the N2c was derived according to the mean stimulus-locked waveform and defined as the time point that reflected the most negative amplitude value between 150-400 ms post-stimulus onset (Loughnane et al., 2016; Brosnan et al., 2023). We calculated N2c amplitude as the mean amplitude within a 10 ms window centred on the N2c's grand average peak (Loughnane et al., 2016; Brosnan et al., 2023). The same was done to calculate peak amplitude and latency of the N2i, but from ipsilateral electrodes. To increase the accuracy of N2c/N2i amplitude and decrease any influence from slow drifts, we subtracted a baseline amplitude up to 180 ms post-target, given the lack of ERP response in that period (Loughnane et al., 2016). To derive measures of CPP onset and peak latency, we first applied a 2 Hz low-pass filter to the stimulus-locked CPP waveform to smooth out noise that might interfere with these calculations. Peak latency was measured as the time point at which the CPP waveform from 400-1000 ms post-stimulus onset (the end of the EEG artifact rejection window) reached its peak amplitude. CPP onset was defined as the timepoint at which the CPP waveform reached half of its peak amplitude.

Additional metrics of build-up rate and peak amplitude were calculated using the response-locked CPP waveform. We first fitted a straight line to each participant's waveform (O'Connell

et al., 2012; Loughnane et al., 2016; Brosnan et al., 2020, 2023) and defined the CPP build-up rate as the slope within a -150 to -50 ms window around the response (Brosnan et al., 2020, 2023; Stefanac et al., 2021). Finally, CPP amplitude was defined as the mean amplitude of the response-locked waveform from -25 to 25ms post-response (Kelly and O'Connell, 2013; Van Kempen et al., 2019; Brosnan et al., 2023).

Imaging Data

We acquired clinical brain imaging data from hospital records for *n*=21 patients (*n*=9 CT, *n*=12 MRI. For those with MRI data, we manually selected the image that best demonstrated the lesion (*1 DWI, 7 FLAIR, 2 T2, 2 T1*). Recent research has verified that similar routine clinical imaging data are of sufficient quality to accurately localise established neural correlates in statistical lesion mapping analyses (Moore and Demeyere, 2022; Moore et al., 2023). Lesion masks were derived and processed in line with a standard analysis pipeline (Moore, n.d.). Specifically, lesions were manually delineated on the axial plane of native space scans by a trained expert (MJM) using MRIcron (Rorden et al., 2007). These native-space masks were smoothed at 5mm full width at half maximum in the z-direction, reoriented to the anterior commissure and normalised to 1x1x1 MNI space. This spatial normalisation was completed using Statistical Parametric Mapping (Penny et al., 2007) and standard, age-matched templates (Clinical Toolbox; Rorden et al., 2012). All normalised scans and lesions were visually inspected to ensure accuracy.

Visual inspection of lesion distribution at group level suggested insufficient overlap to support statistical lesion mapping analyses (Moore et al., 2023). For this reason, this study does not aim to draw definitive conclusions about the anatomical correlates of human perceptual decision making after stroke, but instead broadly compares lesion characteristics between groups.

To this end, lesion maps are presented for each patient group in Fig. 1. Individual lesion masks, network disconnection summaries, and cortical integrity statistics can be found in Figures S1 and S2, and Table S3, respectively.

Patient Competency Rating Scale (PCRS)

Self-reported psychosocial functioning was examined using the 30-item PCRS (Prigatano, 1986). Participants rated the ease with which they could perform a range of common activities

(e.g., dressing themselves, or remembering their daily schedule) on a five-point Likert scale from 1 ("Can't do") to 5 ("Can do with ease"). Scores were aggregated such that higher scores suggest higher functioning. The PCRS has been validated for characterising psychosocial functioning following stroke (Barskova and Wilz, 2006).

Experimental Design and Statistical Analyses

Many of the conducted analyses utilised the same structure, investigating the existence of a Group (Control, Left Stroke, Right Stroke) x Target Hemifield (Left, Right) interaction. For RT, N2c amplitude, N2i amplitude and CPP peak amplitude, we used single trial analysis using Linear Mixed Effects (LME) modelling, predicting the given outcome measure with fixed effects of Group and Target Hemifield and random slopes and intercepts for Target Hemifield x Participant. Thus, the equation for those models was the following: [RT/N2c/N2i/CPP] ~ TargetHemifield x Group + (TargetHemifield|Participant). This was the maximal model that could be fitted and permitted individual participant effects to vary, while still revealing group-level effects. Other analyses were conducted on a participant-level to increase signal-to-noise ratio before measurement: N2c peak latency, N2i peak latency, CPP onset latency, CPP peak latency and CPP build-up rate. These analyses were performed using a mixed-effects ANOVA, with factors of Target Hemifield and Group. When using LME, we performed Bonferroni-Holm-adjusted post-hoc analyses comparing Target Hemifield within each Group using further LMEs, whereas when using ANOVA, we performed post-hoc analyses using within group *t*-tests and calculated Bonferroni-Holm-adjusted *p* values to account for multiple comparisons.

Next, for Left and Right Stroke Groups, we calculated Left Hemifield minus Right Hemifield asymmetry indices for both RT and our ERP metrics of interest via the following formula: (Left Target - Right Target)/((Left Target + Right Target)/2). Thus, for RT and ERP latency variables, lower indices denoted earlier timing to left hemifield targets, whereas higher indices reflected earlier timing for right hemifield targets. There was one exception to this strategy for N2c/N2i amplitude asymmetry indices, which were calculated using the following formula: (Left Target - Right Target)((abs(Left Target) + (abs(Right Target))/2). Here, the absolute of the signals was used in the denominator for these indices due the fact that the N2 signals could be negative. As such, for these amplitude metrics, lower indices were indicative of greater (i.e., more negative) N2c/N2i amplitude in response to left hemifield targets, whereas higher indices

denoted greater amplitude in response to right hemifield targets. To ascertain the relationship between these indices, we performed a linear regression, covarying for Stroke Group to ensure that effects were not simply driven by differences between groups.

We followed up these analyses with two serial mediation analyses to investigate whether the effect of Stroke Group on RT asymmetry was mediated via N2c amplitude asymmetry, then CPP onset (and peak latency in a secondary mediation) asymmetry. We performed two, two-stage serial mediations, with Stroke Group as predictor, N2c amplitude asymmetry and CPP onset/CPP peak latency asymmetry as serial mediators, and RT asymmetry as the Dependent Variable.

Finally, we tested the relationship between RT asymmetry and Quality of Life indices, measured by the PCRS. Given that PCRS is an absolute measure, we calculated a slightly different RT asymmetry index which denoted worse contralesional RTs: (Contra Target - Ipsi Target)((Contra Target + Ipsi Target)/2). A lower index here denoted faster RT to targets contralateral to the lesioned hemisphere, whereas a higher index denoted slower RT to contralesional targets, i.e., the effect one might expect post-stroke. We then performed a linear regression of RT asymmetry index on PCRS, again covarying for Stroke Group.

Results

Unilateral Stroke Compromises the Speed of Contralesional Responding

Hit rate on the BRDM task was at ceiling across most participants, suggesting that in general participants did not have any difficulty with the task requirements. Four right hemisphere patients had a hit rate lower than 90% for left hemifield targets. To examine group differences in the timing of perceptual reports across hemifields, we first utilised a linear mixed-effects model (LMM) to examine group and target hemifield differences in RT. RT was measured as the time (in milliseconds) from the onset of target motion to a response. The model included Group (control, left hemisphere patients and right hemisphere patients), Target Hemifield (left and right), and a Group x Target Hemifield interaction as fixed effects, with a random effect to account for within-subject effects. All post-hoc comparisons were Bonferroni-Holm adjusted.

The LMM revealed a significant main effect of Group (F(2,11275)=3.87, p=.02; see Table S1 for all models), but no significant main effect of Target Hemifield (F(1,11275)=2.27, p=.13). Critically, there was a significant interaction between Group and Target Hemifield (F(2,11275)=7.21, p<.001). The interaction effect was driven by the two patient groups who showed significantly slowed responding to contralesional, relative to ipsilesional, stimuli. On average, the right hemisphere patients responded 137 ms more slowly to left compared with right hemifield targets (left: M=794ms, SD=327; right: M=657ms, SD=120; t(3769)=-2.38, p_{corr}=.03, model estimate difference=-136, 95% CI [-248.41 -24.05]), whereas the left hemisphere patients responded 44 ms more slowly to right compared with left hemifield stimuli (left: M=538ms, SD=129; right: M=582ms, SD=147; t(2514)=3.43, p_{corr}=.01, model estimate difference=44.76, 95% CI [16.36 73.16]). There was no significant asymmetry in response times for the controls (left: M=632ms, SD=165; right: M=632ms, SD=130; t(4992)=0.07, p_{corr}=.94, model estimate difference=0.73, 95% CI [-19.57, 21.04]). Overall, these results indicate that lesions to either hemisphere compromise the speed of responses to contralesional stimuli. These results are shown in Fig. 1.

Next, we sought to understand the sequence of neural events that might give rise to the contralesional slowing observed in both stroke patient groups, in order to demonstrate the related signals' causal importance. We hypothesised that contralesional slowing of response times could be influenced by variation in the dynamics of the N2 and/or the CPP.

Impaired Contralateral Target Selection in the Damaged Hemisphere

N2c Amplitude

We computed an LMM based on single-trial estimates of peak amplitude to examine group and target hemifield differences in N2c magnitude. As with RT, the LMM showed a significant Group x Target Hemifield interaction (F(2,8599)=6.25, p<.01; Fig. 2A; Table S1), whereby damage to either hemisphere was associated with reduced amplitudes for contralesional, compared with ipsilesional, stimuli (i.e., attenuated signal in the lesioned hemisphere; Table S1). The right hemisphere patients had 9.96 $\mu V/m^2$ greater N2c amplitude for right, compared with left, hemifield targets (left: M=-8.39, SD=8.99; right: M=-18.34, SD=13.75; t(3131)=2.73, p_{corr}=.027, model estimate difference=-10.02, 95% CI [-17.21,-2.83]), whereas the left

hemisphere patients showed an 7.61μV/m^2 greater (i.e. more negative) N2c amplitude for left relative to right hemifield targets (left: *M*=-19.17, *SD*=8.28; right: *M*=-11.56, *SD*=9.76; *t*(1800)=-3.48, p_{corr}=.01, model estimate difference=8.31, 95% CI [3.08, 13.54]). In contrast, we did not find evidence for a difference in N2c amplitude between left and right hemifield targets for the controls (left: *M*=-19.21, *SD*=13.20; right: *M*=-17.28, *SD*=15.44; *t*(3668)=-0.65, p_{corr}=.52, 95% CI [-4.41, 8.48]). Finally, there was no significant main effect of Group (*F*(2,8599)=1.35, *p*=.26) or Target Hemifield (*F*(1,8599)=0.005, *p*=.99). These results show that unilateral brain damage acquired through stroke negatively impacts the strength of early target selection processes in the damaged hemisphere

Relationship with the timing of perceptual reports

Given evidence that the N2c is predictive of RT in younger(Loughnane et al., 2016) and older adults(Brosnan et al., 2023), we explored whether stroke-related changes in this metric were consequential for behaviour. Specifically, to examine whether this difference indexes task-relevant behaviour in the two stroke groups, we first calculated asymmetry indices (see methods for details). Next, we conducted a multiple regression to examine the relationship between the asymmetry of RT and N2c amplitude in patients, with group included as a covariate. There was a significant positive relationship, whereby higher N2c asymmetries (i.e., lower amplitude for left hemifield targets) were associated with more positive RT asymmetries (i.e., slower RT for left hemifield targets), (F(1,27)=11.84, *p*=.002; Fig. 2C; Table S2). These data demonstrate that stroke disrupts the strength of early target selection processes in the lesioned hemisphere, and that this effect is relevant to downstream behavioural responses.

N2c Peak Latency

Next, we used a two-way mixed-effects ANOVA on participant-level means to examine the effects of Group and Target Hemifield on the peak latency of the N2c (i.e., the time from stimulus onset until the peak amplitude of the average waveform). There were no significant main effects of Group (*F*(2,54)=0.50, *p*=.61) or Target Hemifield (*F*(1,54)=0.08, *p*=.78), and no significant interaction effect between Group and Target Hemifield (*F*(2,54)=-.09, *p*=.91). As such, and in contrast to the differences in strength of the N2c component post-stroke described above, we did not find evidence for altered timing of early target selection processes following unilateral damage to the brain.

Impaired Ipsilesional Target Selection specifically following Right Hemisphere Damage

N2i Amplitude

To examine group and target hemifield differences in the magnitude of the ipsilateral target selection signal, N2i(Loughnane et al., 2016), we computed an LMM based on single-trial estimates of peak amplitude. There was a significant Group x Target Hemifield interaction ($F(2,8599)=4.43$, $p=.01$; Fig. 2B; Table S1). Controls (left: $M=-6.22$ μV/m^2, $SD=4.82$; right: $M=-11.43$ μV/m^2, $SD=4.82$) showed a significantly stronger right hemisphere N2i compared with the left hemisphere ($t(3668)=3.23$, $p_{corr}=.002$, model estimate difference=2.38, 95% CI [0.88, 3.88]), consistent with previous work showing that the N2i is right lateralised in healthy individuals(Loughnane et al., 2016). Similar to the controls, the left hemisphere patients had a stronger N2i in the right hemisphere (left: $M=-5.43$ μV/m^2, $SD=3.42$; right: $M=-12.47$ μV/m^2, $SD=3.42$); $t(1800)=4.16$, $p_{corr}=.001$, model estimate difference=3.52, 95% CI [1.53, 5.51]). In contrast to the other two groups, we did not find evidence for a difference across hemispheres for the right hemisphere patients (left: $M=-6.76$ μV/m^2, $SD=6.67$; right: $M=-6.49$ μV/m^2, $SD=6.99$; $t(3131)=-0.07$, $p=.94$, model estimate difference=-0.078 95% CI [-2.05, 1.90]). These results thus reflect a strong right-hemisphere dominance of the N2i in neurologically healthy individuals, and patients with left hemisphere damage, which is absent in patients with right hemisphere lesions.

Relationship with the timing of perceptual reports

Consistent with our approach for the N2c, we next conducted a multiple regression to examine the relationship between the asymmetry of RT and N2i amplitude in our patients, with Group included as a covariate. We did not find evidence for a relationship between the two ($F(1,27)=0.04$, $p=.85$; Fig. 2C; Table S2). Taken together, these results demonstrate that the typical right lateralisation of the N2i is reduced in right hemisphere stroke, but we did not find evidence to suggest that this impacts behaviour.

N2i Peak Latency

We subsequently employed a two-way mixed-effects ANOVA on participant-level means to examine the effects of Group and Target Hemifield on the peak latency of the N2i. As observed

with the N2c, there were no significant main effects of Group (F(2,54)=0.36, p=.70) or Target Hemifield (F(1,54)=1.95, p=.17), and no significant interaction effect between Group and Target Hemifield (F(2,54)=0.14, p=.87).Together, these data do not provide evidence that the timing of ipsilateral target selection ERPs is affected following unilateral stroke

Delayed CPP for Stimuli in the Contralesional Hemifield

Stimulus-Locked Signal

Two-way mixed ANOVAs were used to investigate differences in onset and peak latency of evidence accumulation rates between groups and target hemifields.

CPP Onset

There was a significant Group x Target Hemifield interaction for CPP onset, F(2,53)=11.30, p<.001. Bonferroni-Holm adjusted post-hoc analyses revealed that the right hemisphere patients (t(16)=3.22, p_{corr}<.01) had a later onset of evidence accumulation for left, compared with right hemifield targets. We did not find evidence for a difference in CPP onset for left hemisphere patients (t(11)=-2.45, p_{corr}=.06), or controls (t(26)=-1.31, p_{corr}=.20). There were no significant main effects of Group (F(2,53)=0.11, p=.90) or Target Hemifield (F(1,53)=0.60, p=.44).

CPP Peak Latency

Similar results were found for the peak latency of the CPP; There were no significant main effects of Group (F(2,54)=0.03, p=.97) or Target Hemifield (F(1,54)=1.26, p=.27), but there was a significant interaction (F(2,54)=6.34, p<.01), again driven by differential target hemifield effects as a function of stroke group. For right hemisphere patients, left hemifield targets elicited a later CPP peak compared with right hemifield targets (t(16)=2.69, p_{corr}<.05). We did not find evidence for differences in CPP peak latency as a function of target hemifield in the left hemisphere patients (t(11)=-2.32, p_{corr}=.08), or controls (t(26)=0.66, p_{corr}=.52).

We further examined the relevance of these signals to task-related RT asymmetry exclusively in the stroke groups using two multiple linear regressions (one for each of CPP onset and CPP peak latency asymmetries), with Group included as a covariate. RT asymmetry was related to both CPP onset asymmetry and CPP peak latency asymmetry, such that later onsets (F(1,27)=20.76, p<.001) and peaks (F(1,27)=53.54, p<.001) predicted slower behavioural

responses. Overall, evidence accumulation in the right hemisphere stroke group was slower to begin and end for contralesional, compared with ipsilesional, stimuli. As per findings in healthy adults (O'Connell et al., 2012; Brosnan et al., 2023), markers of delayed evidence accumulation were found to predict slowed responding in both stroke groups (shown Fig. 3).

Response-Locked Signal

We examined group and target hemifield differences in CPP slope using a two-way mixed ANOVA, and peak amplitude using an LMM with fixed effects of Group, Target Hemifield, and a Group x Target Hemifield interaction. There was no significant main effect of Group ($F(2,55)=0.17$, $p=.85$) or Target Hemifield ($F(1,55)=1.29$, $p=.26$), nor a significant Group x Target Hemifield interaction for the CPP slope ($F(2,54)=0.73$, $p=.48$). Similarly, the interaction effect of Group x Target Hemifield was not significant for CPP peak amplitude ($F(2,11091)=2.45$, $p=.09$), nor were the main effects of Group ($F(2,11091)=2.42$, $p=.09$) or Hemifield ($F(1,11091)=2.85$, $p=.09$). Overall, stroke did not appear to alter the dynamics of the response-locked CPP, suggesting that evidence is accumulated at similar rates in contralesional and ipsilesional hemispheres.

Neurophysiological Asymmetries Mediate the Relationship Between Stroke Hemisphere and RT Asymmetry

The findings above suggest that slowed contralesional responding is indexed by diminished markers of contralateral target selection (N2c) and delayed evidence accumulation (CPP). Given previous work demonstrating that these ERPs represent an interrelated temporal sequence of events (Loughnane et al., 2016), we sought to determine whether they could serially mediate the relationship between stroke hemisphere and RT asymmetry. To test this possibility, we performed a mediation analysis, whereby the degree to which RT asymmetry is predicted by stroke hemisphere is mediated serially by the N2c, followed by the CPP onset. Mediation analyses suggested a full mediation of stroke hemisphere on RT asymmetry via both N2c amplitude and CPP onset asymmetries (indirect effect=0.08, $p=.04$, 95% CI [0.003, 0.15]). A similar mediation was found when the model was repeated with CPP peak latency asymmetry instead of CPP onset (indirect effect=0.14, $p<.01$, 95% CI [.04, .25]). Full mediation results are presented diagrammatically in Fig. 4.

Collectively, these findings characterise the nature and temporal sequence of discrete neural events that give rise to contralesional slowing after stroke. Specifically, we provide evidence for a mechanism whereby weakened target selection signals (N2c asymmetry) due to stroke delay time-to-threshold of evidence accumulation (CPP onset and peak latency asymmetries) and thence slow contralesional RT.

Asymmetries in Response Time Predict Poorer Everyday Functioning

Finally, to determine whether the behavioural asymmetry described above has relevance to daily function following stroke, we used a multiple linear regression with an asymmetry measure of task RT (where greater RT asymmetries indicate slower responses to contralesional stimuli, regardless of lesion side; see Materials and methods) as a predictor of PCRS scores, with stroke side as a covariate. There was no significant relationship between lesion volume and RT (r=0.17, p=.49) or PCRS score (r=-.31, p=.21) and thus lesion size was not included as a covariate in these analyses.

There was a significant, negative relationship between RT asymmetry on the BRDM task and everyday functioning, such that slower responses to contralesional targets predicted poorer everyday functioning (F(1,24)=5.67, p=.03). Given this result, we conducted additional, exploratory analyses to examine whether asymmetries in our neurophysiological metrics were related to everyday function. There was marginal evidence for the relevance of CPP parameters to post-stroke daily function, however this was not robust to correction for multiple comparisons (see Text S1 and Figure S3).

Taken together, these results suggest that the BRDM task is indexing a facet of cognition that has real-life implications for daily functioning post-stroke.

Discussion

We leveraged an integrated EEG/perceptual decision-making paradigm in stroke patients to identify the causal contribution of the target selective N2 signal to behaviour. Results revealed that the relationship between lesion hemisphere and spatial RT bias was mediated by attenuation of the N2c in response to contralesional stimuli. Furthermore, we found that this

relationship was mediated by delayed evidence accumulation as indicated by a slower onset and thus time-to-threshold of the CPP. To our knowledge, this is the first time that a temporal sequence of discrete and well-described neural events, i.e. the target-selective N2c and decision-related CPP, has been causally linked to behaviour in humans.

Unilateral lesions selectively weakened the contralateral N2 in the affected hemisphere and subsequently slowed responses. The N2c traces the early selection of goal-relevant targets in uncertain environments and increases proportionally to the quality and availability of sensory evidence (Loughnane et al., 2016). Our results show that the N2c amplitude was weaker in the absence of any difference of N2c latency. This may suggest that while timely onset of early target selection was preserved, this was accompanied by a distinct deficit in the attentional selection of the relevant stimulus. This accords with previous correlational work relating the N2c to behaviour (Loughnane et al., 2016; Newman et al., 2017), where a weaker N2c predicted slower responses (Van Kempen et al., 2019). Here we build on this work to show that hemisphere-specific damage to the brain is causally associated with weaker N2c signals with subsequent impacts on behaviour (slower responses).

In addition, our observations highlight the consequences of weaker target selection signals for downstream processes (perceptual decision formation), thereby establishing a causal chain of events underpinning variability in behaviour. Specifically, we highlight a potential pathway through which the target selective N2c can impact response times. Stroke-related contralesional slowing was additionally correlated with the time of onset and peak of the CPP, an established marker of evidence accumulation (O'Connell et al., 2012; Philiastides et al., 2014; Murphy et al., 2015; Twomey et al., 2016; Spitzer et al., 2017; McGovern et al., 2018; Steinemann et al., 2018b; Herding et al., 2019; van Vugt et al., 2019b; von Lautz et al., 2019; Brosnan et al., 2020, 2023; Ruesseler et al., 2023). Previous studies on post-stroke contralesional slowing have observed a delayed P300 (Lhermitte et al., 1985; Priftis et al., 2008; Lasaponara et al., 2018) – an ERP that shares many features with the CPP (O'Connell et al., 2012; Twomey et al., 2015). Our findings extend this in three critical ways. First, our models suggested that the timing of the CPP mediated the relationship between N2c amplitude and RT, and thus demonstrate that delayed evidence accumulation is driven by earlier disruption of target selection. This establishes a causal role for early target selection signals such as the N2c in facilitating and modulating downstream evidence accumulation processes (Loughnane et al., 2016). Second,

we show that asymmetry in the timing of evidence accumulation onset directly related to variance in performance stems from a weaker asymmetry of the N2c, thereby increasing the certainty with which these can be attributed as causal. Finally, we demonstrate a dissociation between the time taken to begin evidence accumulation, and the rate at which evidence is sampled: whereas the CPP begins later for contralesional stimuli following stroke, we did not find evidence to suggest that stroke compromises the rate at which the brain accumulates evidence. Thus, following stroke, decision formation is equally efficient for stimuli presented to ipsilesional and contralesional hemifields, but these processes occur later for contralesional stimuli. Collectively, these data suggest a plausible causal temporal pathway by which unilateral stroke dampens the early selection of sensory stimuli in the contralesional hemifield, and subsequently delays the onset (and thus peak) of evidence accumulation, thereby slowing responses.

Another benefit of our paradigm was the ability to parse out contralateral and ipsilateral target selection, via the elimination of VEPs in response to sudden-onset stimuli. As noted above, our results suggest that the core deficit following stroke stems from reduced stimuli salience in the contralesional hemifield. Notably, right hemisphere patients demonstrated additional attenuation of the ipsilateral N2 in the affected hemisphere. One possibility is that this effect is specific to lesions in the right hemisphere due to inter-hemispheric differences in the distribution of attention networks (see Corbetta and Shulman, 2002). There was, however, no evidence that disruptions to ipsilateral target selection meaningfully impacted behaviour, reaffirming the relative importance of contralateral, as opposed to ipsilateral, visual processing (Loughnane et al., 2016; Newman et al., 2017).

Between-hemifield asymmetries in the timing of responses were correlated with daily function, suggesting that the asymmetries displayed here meaningfully influence behaviour. Asymmetrical sensory processing has been previously shown to deleteriously affect performance of everyday activities such as driving (Van Kessel et al., 2013). This may be attributable to the relationship between neural decision-making and higher cognitive functioning (Shadlen and Kiani, 2013) such that hemisphere-specific alterations to the brain's capacity to select, process and thus respond to relevant stimuli may more broadly impact one's ability to function within one's environment. Exploratory analyses exploring the relationship between the CPP and everyday functioning showed marginal support for this hypothesis,

though this effect was not robust to multiple comparisons correction and will require replication. Importantly, many of our participants were well beyond the expected critical time points of functional recovery post-stroke (Jørgensen et al., 1995; Xi et al., 2006; Bernhardt et al., 2017; Hankey, 2017), indicating that these impacts are persistent and resistant to current rehabilitation methods.

Notably, asymmetries in the neurophysiological signatures of selection and decision processes appeared to be robust determinants of behavioural asymmetries across participants, independent of stroke hemisphere and time since stroke. Further, the lesions of our sample were heterogeneous, with diverse network disconnection profiles and stroke aetiologies, and yet commonalities emerged. Such generalisability speaks to the relevance of neural perceptual decision-making to broader cognition, and the involvement of large, interconnected networks in decision-making (Gherman et al., n.d.; Shadlen and Kiani, 2013; Brosnan et al., 2020). Collectively, our framework captures behavioural and neural metrics that are relevant to functioning and are generalisable across a wide range of lesions. This is notable, as lesion characteristics are often imperfect predictors of outcome, necessitating complex multivariate analyses to achieve suboptimal structure-function alignment (see Price et al., 2017 for discussion of these issues). Given the relevance of these neurophysiological metrics to the behaviour and broader functioning, a focus of future work will be to establish whether they have utility in clinical assessment or management over and above that of existing procedures.

In evaluating these results, we acknowledge the inherent simplicity of the BRDM task, as evidenced by the relatively strong performance of our clinical sample. This simplicity raises the question of whether the influence of sensory-driven processes (i.e., the N2c) shown here would extend to more complex tasks that are more dependent on higher-order cognitive processing. However, the BRDM has demonstrated capacity to elicit meaningful variation in both evidence accumulation signals (CPP) and behaviour (RT), even though hit rate (accuracy) is at ceiling (e.g., Newman et al., 2017; Brosnan et al., 2020, 2023). Correspondingly, in this cohort of stroke patients we capture meaningful variability in both neural and behavioural indices of decision making, suggesting adequate engagement of higher-order processing. Despite this, our mediation analyses suggest that the N2c is preceding and determining the trajectory of evidence accumulation and subsequent decision speed. This suggests that the role of sensory-driven processes has a cascading influence on more complex cognitive operations

to subsequently guide decision making. Future work could further test this causal trajectory by combining our EEG approach with additional tasks which necessitate greater cognitive demands.

An additional consideration is the risk of bias within our sample conferred by the exclusion of a large proportion of the recruited participants. Most notably, patients unable to complete sufficient BRDM trials and those with bilateral lesions on neuroimaging review were not included. Cognitive, physical and/or visual disabilities are extremely common in stroke patients (Sun et al., 2014; Carmo et al., 2015), and the experience of one stroke increases the risk of another in the following five years ninefold (Burn et al., 1994). Although such selectivity has enabled insights into the impact of unilateral stroke, as a result our cohort accounts for only a small subset of stroke patients, limiting the generalisability of our results. Positively, our findings of dysfunctional target selection and evidence accumulation signals align with previous electrophysiological (Lhermitte et al., 1985; Tachibana et al., 1993; Priftis et al., 2008; e.g., Lasaponara et al., 2018) and limited theoretical modelling studies (Ulrichsen et al., 2020), although significant methodological differences and variability in results makes direct comparison challenging. Our findings will benefit from replication in larger, more heterogeneous samples of stroke survivors.

In summary, here we apply an integrated EEG paradigm to fractionate the key neural determinants of perceptual decision-making after stroke. We define a temporal sequence of neurophysiological events from weakened attentional selection in the damaged hemisphere through to delayed evidence accumulation, which culminate in slowed perceptual decision-making for contralesional stimuli. These results were robust to heterogeneity in the lesion characteristics of our sample. Taken together, our results point to a causal role for contralateral target selection signals in modulating downstream decision-making and behavioural processes.

Data availability

Ethical clearance to make data publicly available was not obtained for all participating sites. Custom MATLAB scripts used to process and analyse EEG data are available at https://osf.io/mvehu/?view_only=12aef65f46e246fcb94b1e8bd6dba040.

Funding

This work was funded by an NHMRC Project Grant to MAB, JBM and RGO (#1140707); Australian Research Council Grants DP150100986 and DP180102066 to M.A.B and R.G.O; a European Commission Grant #844246 and a Cullen Junior Research Fellowship at Corpus Christi College, University of Oxford, to M.B.B.; a National Institute for Health Research Oxford Health Biomedical Research Center and Wellcome Centre for Integrative Neuroimaging Wellcome Trust Grant 203139/Z/16/Z; an Australian NHMRC Senior Research Fellowship (Level B; APP1154378) to M.A.B.; a European Research Council Grant #865474 to R.G.O.; an Australian Research Council Grant FTFT220100294 to T.T.-J.C.; a National Institute for Health Research Advanced Fellowship NIHR302224 to N.D.; an NHMRC Investigator Grant (Leadership 3; GNT2010141) to J.B.M.; an NHMRC Ideas grant (APP1186955) to D.R.; and an Australian Government Research Training Program (RTP) Scholarship to D.J.P.

Competing interests

The authors report no competing interests.

Supplementary material

Supplementary material is available .

References

Afacan-Seref K, Steinemann NA, Blangero A, Kelly SP (2018) Dynamic Interplay of Value and Sensory Information in High-Speed Decision Making. Current Biology 28:795-802.e6.

Ballard C, Stephens S, Kenny RA, Kalaria R, Tovee M, O'Brien J (2003) Profile of Neuropsychological Deficits in Older Stroke Survivors without Dementia. Dement

Geriatr Cogn Disord 16:52–56 Available at: https://dx.doi.org/10.1159/000069994 [Accessed July 19, 2023].

Barskova T, Wilz G (2006) Psychosocial functioning after stroke: Psychometric properties of the patient competency rating scale. Brain Inj 20:1431–1437.

Bender MB (2011) Disorders in Perception: With Particular Reference to the Phenomena of Extinction and Displacement. Charles C Thomas Publisher.

Bernhardt J, Hayward KS, Kwakkel G, Ward NS, Wolf SL, Borschmann K, Krakauer JW, Boyd LA, Carmichael ST, Corbett D, Cramer SC (2017) Agreed Definitions and a Shared Vision for New Standards in Stroke Recovery Research: The Stroke Recovery and Rehabilitation Roundtable Taskforce. Neurorehabil Neural Repair 31:793–799.

Brainard DH (1997) The Psychophysics Toolbox. Spat Vis 10:433–436.

Brosnan MB, Pearce DJ, O'Neill MH, Loughnane GM, Fleming B, Zhou SH, Chong T, Nobre AC, O'Connell RG, Bellgrove MA (2023) Evidence Accumulation Rate Moderates the Relationship between Enriched Environment Exposure and Age-Related Response Speed Declines. Journal of Neuroscience 43:6401–6414 Available at: https://www.jneurosci.org/content/43/37/6401 [Accessed November 13, 2023].

Brosnan MB, Sabaroedin K, Silk T, Genc S, Newman DP, Loughnane GM, Fornito A, O'Connell RG, Bellgrove MA (2020) Evidence accumulation during perceptual decisions in humans varies as a function of dorsal frontoparietal organization. Nat Hum Behav 4:844–855 Available at: https://www.nature.com/articles/s41562-020-0863-4 [Accessed June 26, 2023].

Burn J, Dennis M, Bamford J, Sandercock P, Wade D, Warlow C (1994) Long-term risk of recurrent stroke after a first-ever stroke. The Oxfordshire Community Stroke Project. Stroke 25:333–337 Available at: https://pubmed.ncbi.nlm.nih.gov/8303740/ [Accessed March 5, 2025].

Carmo JF do, Morelato RL, Pinto HP, Oliveira ERA de (2015) Disability after stroke: a systematic review. Fisioterapia em Movimento 28:407–418 Available at: https://www.scielo.br/j/fm/a/DdzHv9MrgFp7pF4tsdvRYCv/?lang=en [Accessed March 5, 2025].

Corbetta M, Shulman GL (2002) Control of goal-directed and stimulus-driven attention in the brain. Nat Rev Neurosci 3:201–215 Available at: https://www.nature.com/articles/nrn755 [Accessed October 20, 2023].

Cornelissen FW, Peters EM, Palmer J (2002) The Eyelink Toolbox: Eye tracking with MATLAB and the Psychophysics Toolbox. Behavior Research Methods, Instruments, and Computers 34:613–617 Available at: https://link.springer.com/article/10.3758/bf03195489 [Accessed July 20, 2023].

De Lange FP, Jensen O, Dehaene S (2010) Accumulation of Evidence during Sequential Decision Making: The Importance of Top–Down Factors. Journal of Neuroscience 30:731–738 Available at: https://www.jneurosci.org/content/30/2/731 [Accessed September 22, 2024].

Delorme A, Makeig S (2004) EEGLAB: An open source toolbox for analysis of single-trial EEG dynamics including independent component analysis. J Neurosci Methods 134:9–21 Available at: https://pubmed.ncbi.nlm.nih.gov/15102499/ [Accessed July 20, 2023].

Demeyere N, Riddoch MJ, Slavkova ED, Bickerton WL, Humphreys GW (2015) The Oxford Cognitive Screen (OCS): validation of a stroke-specific short cognitive screening tool. Psychol Assess 27:883–894 Available at: https://pubmed.ncbi.nlm.nih.gov/25730165/ [Accessed July 20, 2023].

Derosiere G, Thura D, Cisek P, Duque J (2019) Society for the Neural Control of Movement: Motor cortex disruption delays motor processes but not deliberation about action choices. J Neurophysiol 122:1566 Available at: /pmc/articles/PMC6843092/ [Accessed September 22, 2024].

Ding L, Gold JI (2012) Neural correlates of perceptual decision making before, during, and after decision commitment in monkey frontal eye field. Cereb Cortex 22:1052–1067 Available at: https://pubmed.ncbi.nlm.nih.gov/21765183/ [Accessed September 22, 2024].

Donner TH, Siegel M, Fries P, Engel AK (2009) Report Buildup of Choice-Predictive Activity in Human Motor Cortex during Perceptual Decision Making. Current Biology 19:1581–1585.

Eimer M (1996) The N2pc component as an indicator of attentional selectivity. Electroencephalogr Clin Neurophysiol 99:225–234.

Eimer M (2014) The neural basis of attentional control in visual search. Trends Cogn Sci 18:526–535 Available at: https://pubmed.ncbi.nlm.nih.gov/24930047/ [Accessed September 22, 2024].

Fish S, Toumaian M, Pappa E, Davies TJ, Tanti R, Saville CWN, Theleritis C, Economou M, Klein C, Smyrnis N (2018) Modelling reaction time distribution of fast decision tasks in schizophrenia: Evidence for novel candidate endophenotypes. Psychiatry Res 269:212–220 Available at: https://pubmed.ncbi.nlm.nih.gov/30153599/ [Accessed September 22, 2024].

Fleming SM, Maniscalco B, Ko Y, Amendi N, Ro T, Lau H (2015) Action-Specific Disruption of Perceptual Confidence. Psychol Sci 26:89–98 Available at: https://journals.sagepub.com/doi/full/10.1177/0956797614557697 [Accessed September 22, 2024].

Fosco WD, White CN, Hawk LW (2017) Acute Stimulant Treatment and Reinforcement Increase the Speed of Information Accumulation in Children with ADHD. J Abnorm Child Psychol 45:911–920 Available at: https://pubmed.ncbi.nlm.nih.gov/27787672/ [Accessed September 22, 2024].

Ghaderi-Kangavari A, Parand K, Ebrahimpour R, Nunez MD, Amani Rad J (2023) How spatial attention affects the decision process: looking through the lens of Bayesian hierarchical diffusion model & EEG analysis. Journal of Cognitive Psychology 35:456–479 Available at: https://www.tandfonline.com/doi/abs/10.1080/20445911.2023.2187714 [Accessed December 11, 2023].

Gherman S, Markowitz N, Tostaeva G, Espinal E, Mehta AD, O RG, Kelly SP, Bickel S (n.d.) Intracranial electroencephalography reveals effector-independent evidence accumulation dynamics in multiple human brain regions. Available at: https://doi.org/10.1101/2023.04.10.536314 [Accessed June 26, 2023].

Hankey GJ (2017) Stroke. The Lancet 389:641–654.

Hanks TD, Ditterich J, Shadlen MN (2006) Microstimulation of macaque area LIP affects decision-making in a motion discrimination task. Nat Neurosci 9:682–689 Available at: https://pubmed.ncbi.nlm.nih.gov/16604069/ [Accessed September 22, 2024].

Heitz RP, Schall JD (2012) Neural mechanisms of speed-accuracy tradeoff. Neuron 76:616–628 Available at: https://pubmed.ncbi.nlm.nih.gov/23141072/ [Accessed September 22, 2024].

Herding J, Ludwig S, von Lautz A, Spitzer B, Blankenburg F (2019) Centro-parietal EEG potentials index subjective evidence and confidence during perceptual decision making. Neuroimage 201:116011.

Hickey C, Di Lollo V, McDonald JJ (2009) Electrophysiological indices of target and distractor processing in visual search. J Cogn Neurosci 21:760–775 Available at: https://pubmed.ncbi.nlm.nih.gov/18564048/ [Accessed September 22, 2024].

Huang YT, Georgiev D, Foltynie T, Limousin P, Speekenbrink M, Jahanshahi M (2015) Different effects of dopaminergic medication on perceptual decision-making in Parkinson's disease as a function of task difficulty and speed–accuracy instructions. Neuropsychologia 75:577–587.

Hurford R, Charidimou A, Fox Z, Cipolotti L, Werring DJ (2013) Domain-specific trends in cognitive impairment after acute ischaemic stroke. J Neurol 260:237–241 Available at: https://link.springer.com/article/10.1007/s00415-012-6625-0 [Accessed July 19, 2023].

Johansson B, Rönnbäck L (2012) Mental fatigue and cognitive impairment after an almost neurological recovered stroke. ISRN Psychiatry 2012:1–7 Available at: https://pubmed.ncbi.nlm.nih.gov/23738208/ [Accessed July 19, 2023].

Jørgensen HS, Nakayama H, Raaschou HO, Vive-Larsen J, Støier M, Olsen TS (1995) Outcome and time course of recovery in stroke. Part II: Time course of recovery. The copenhagen stroke study. Arch Phys Med Rehabil 76:406–412.

Kappenman ES, Luck SJ eds. (2011) The Oxford Handbook of Event-Related Potential Components. Oxford University Press. Available at: https://academic.oup.com/edited-volume/34558 [Accessed September 22, 2024].

Katz LN, Yates JL, Pillow JW, Huk AC (2016) Dissociated functional significance of decision-related activity in the primate dorsal stream. Nature 2016 535:7611 535:285–288 Available at: https://www.nature.com/articles/nature18617 [Accessed September 22, 2024].

Kayser J, Tenke CE (2006) Principal components analysis of Laplacian waveforms as a generic method for identifying ERP generator patterns: II. Adequacy of low-density estimates. Clinical Neurophysiology 117:369–380.

Kelly SP, O'Connell RG (2013) Internal and External Influences on the Rate of Sensory Evidence Accumulation in the Human Brain. Journal of Neuroscience 33:19434–19441 Available at: https://www.jneurosci.org/content/33/50/19434 [Accessed June 26, 2023].

Kim JN, Shadlen MN (1999) Neural correlates of a decision in the dorsolateral prefrontal cortex of the macaque. Nat Neurosci 2:176–185 Available at: https://pubmed.ncbi.nlm.nih.gov/10195203/ [Accessed September 22, 2024].

Kiss M, Van Velzen J, Eimer M (2008) The N2pc component and its links to attention shifts and spatially selective visual processing. Psychophysiology 45:240–249 Available at: https://onlinelibrary.wiley.com/doi/full/10.1111/j.1469-8986.2007.00611.x [Accessed June 27, 2023].

Lasaponara S, D'Onofrio M, Pinto M, Dragone A, Menicagli D, Bueti D, De Lucia M, Tomaiuolo F, Doricchi F (2018) EEG correlates of preparatory orienting, contextual updating and inhibition of sensory processing in left spatial neglect. Journal of Neuroscience 38:3792–3808 Available at: https://www.jneurosci.org/content/early/2018/03/19/JNEUROSCI.2817-17.2018 [Accessed June 27, 2023].

Lhermitte F, Turell E, Lebrigand D, Chain F (1985) Unilateral Visual Neglect and Wave P 300: A Study of Nine Cases With Unilateral Lesions of the Parietal Lobes. Arch Neurol 42:567–573 Available at: https://jamanetwork.com/journals/jamaneurology/fullarticle/584244 [Accessed June 27, 2023].

Loughnane GM, Newman DP, Bellgrove MA, Lalor EC, Kelly SP, O'Connell RG (2016) Target Selection Signals Influence Perceptual Decisions by Modulating the Onset and

Rate of Evidence Accumulation. Curr Biol 26:496–502 Available at: https://pubmed.ncbi.nlm.nih.gov/26853360/ [Accessed June 27, 2023].

Luck SJ (2012) Electrophysiological correlates of the focusing of attention within complex visual scenes: N2pc and related ERP components. In: The Oxford handbook of event-related potential component (Luck SJ, Kappenman ES, eds), pp 329–360. Oxford University Press. Available at: https://psycnet.apa.org/record/2013-01016-012 [Accessed September 22, 2024].

Luck SJ, Hillyard SA (1994) Electrophysiological correlates of feature analysis during visual search. Psychophysiology 31:291–308 Available at: https://pubmed.ncbi.nlm.nih.gov/8008793/ [Accessed September 22, 2024].

Mante V, Sussillo D, Shenoy K V., Newsome WT (2013) Context-dependent computation by recurrent dynamics in prefrontal cortex. Nature 2013 503:7474 503:78–84 Available at: https://www.nature.com/articles/nature12742 [Accessed September 22, 2024].

Mazza V, Turatto M, Caramazza A (2009) An electrophysiological assessment of distractor suppression in visual search tasks. Psychophysiology 46:771–775 Available at: https://onlinelibrary.wiley.com/doi/full/10.1111/j.1469-8986.2009.00814.x [Accessed September 22, 2024].

McGovern DP, Hayes A, Kelly SP, O'Connell RG (2018) Reconciling age-related changes in behavioural and neural indices of human perceptual decision-making. Nat Hum Behav 2:955–966.

Moore MJ (n.d.) A Practical Guide to Lesion Symptom Mapping. Available at: https://psyarxiv.com/2jxr9/ [Accessed August 1, 2023].

Moore MJ, Demeyere N (2022) Lesion symptom mapping of domain-specific cognitive impairments using routine imaging in stroke. Neuropsychologia 167 Available at: https://pubmed.ncbi.nlm.nih.gov/35041840/ [Accessed August 1, 2023].

Moore MJ, Jenkinson M, Griffanti L, Huygelier H, Gillebert CR, Demeyere N (2023) A comparison of lesion mapping analyses based on CT versus MR imaging in stroke. Neuropsychologia 184:108564.

Moore MJ, Milosevich E, Beisteiner R, Bowen A, Checketts M, Demeyere N, Fordell H, Godefroy O, Laczó J, Rich T, Williams L, Woodward-Nutt K, Husain M (2022) Rapid screening for neglect following stroke: A systematic search and European Academy of Neurology recommendations. Eur J Neurol 29:2596–2606 Available at: https://onlinelibrary.wiley.com/doi/full/10.1111/ene.15381 [Accessed August 1, 2023].

Murphy PR, Robertson IH, Harty S, O'Connell RG (2015) Neural evidence accumulation persists after choice to inform metacognitive judgments. Elife 4:e11946.

Nasreddine ZS, Phillips NA, Bédirian V, Charbonneau S, Whitehead V, Collin I, Cummings JL, Chertkow H (2005) The Montreal Cognitive Assessment, MoCA: A Brief Screening Tool For Mild Cognitive Impairment. J Am Geriatr Soc 53:695–699 Available at: https://onlinelibrary.wiley.com/doi/full/10.1111/j.1532-5415.2005.53221.x [Accessed July 20, 2023].

Newman DP, Loughnane GM, Kelly SP, O'Connell RG, Bellgrove MA (2017) Visuospatial Asymmetries Arise from Differences in the Onset Time of Perceptual Evidence Accumulation. The Journal of Neuroscience 37:3378 Available at: /pmc/articles/PMC6596774/ [Accessed July 20, 2023].

Newsome WT, Britten KH, Movshon JA (1989) Neuronal correlates of a perceptual decision. Nature 341:52–54 Available at: https://pubmed.ncbi.nlm.nih.gov/2770878/ [Accessed July 20, 2023].

Nunez MD, Gosai A, Vandekerckhove J, Srinivasan R (2019) The latency of a visual evoked potential tracks the onset of decision making. Neuroimage 197:93–108 Available at: https://pubmed.ncbi.nlm.nih.gov/31028925/ [Accessed June 27, 2023].

O'Connell RG, Dockree PM, Kelly SP (2012) A supramodal accumulation-to-bound signal that determines perceptual decisions in humans. Nat Neurosci 15:1729–1735 Available at: https://www.nature.com/articles/nn.3248 [Accessed June 26, 2023].

O'Connell RG, Kelly SP (2021) Neurophysiology of Human Perceptual Decision-Making. Annu Rev Neurosci 44:495–516 Available at: https://pubmed.ncbi.nlm.nih.gov/33945693/ [Accessed September 22, 2024].

Pelli DG (1997) The VideoToolbox software for visual psychophysics: Transforming numbers into movies. Spat Vis 10:437–442 Available at: https://nyuscholars.nyu.edu/en/publications/the-videotoolbox-software-for-visual-psychophysics-transforming-n [Accessed July 20, 2023].

Penny W, Friston K, Ashburner J, Kiebel S, Nichols T (2007) Statistical Parametric Mapping: The Analysis of Functional Brain Images. Statistical Parametric Mapping: The Analysis of Functional Brain Images.

Philiastides MG, Heekeren HR, Sajda P (2014) Human Scalp Potentials Reflect a Mixture of Decision-Related Signals during Perceptual Choices. The Journal of Neuroscience 34:16877 Available at: /pmc/articles/PMC4261107/ [Accessed November 13, 2023].

Price CJ, Hope TM, Seghier ML (2017) Ten problems and solutions when predicting individual outcome from lesion site after stroke. Neuroimage 145:200 Available at: /pmc/articles/PMC5154378/ [Accessed September 5, 2023].

Priftis K, Piccione F, Giorgi F, Meneghello F, Umiltà C, Zorzi M (2008) Lost in number space after right brain damage: A neural signature of representational neglect. Cortex 44:449–453.

Prigatano GP (1986) Neuropsychological rehabilitation after brain injury (Prigatano GP, ed). Johns Hopkins University Press. Available at: https://cir.nii.ac.jp/crid/1130000797026384896 [Accessed July 20, 2023].

Rorden C, Bonilha L, Fridriksson J, Bender B, Karnath HO (2012) Age-specific CT and MRI templates for spatial normalization. Neuroimage 61:957–965 Available at: https://pubmed.ncbi.nlm.nih.gov/22440645/ [Accessed August 1, 2023].

Rorden C, Karnath HO, Bonilha L (2007) Improving lesion-symptom mapping. J Cogn Neurosci 19:1081–1088 Available at: https://pubmed.ncbi.nlm.nih.gov/17583985/ [Accessed August 1, 2023].

Ruesseler M, Weber LA, Marshall TR, O'Reilly J, Hunt LT (2023) Quantifying decision-making in dynamic, continuously evolving environments. Elife 12.

Rungratsameetaweemana N, Itthipuripat S, Salazar A, Serences JT (2018) Expectations Do Not Alter Early Sensory Processing during Perceptual Decision-Making. Journal of

Neuroscience 38:5632–5648 Available at: https://www.jneurosci.org/content/38/24/5632 [Accessed September 22, 2024].

Shadlen MN, Kiani R (2013) Decision Making as a Window on Cognition. Neuron 80:791–806.

Shadlen MN, Newsome WT (2001) Neural basis of a perceptual decision in the parietal cortex (area LIP) of the rhesus monkey. J Neurophysiol 86:1916–1936 Available at: https://pubmed.ncbi.nlm.nih.gov/11600651/ [Accessed April 29, 2024].

Spitzer B, Waschke L, Summerfield C (2017) Selective overweighting of larger magnitudes during noisy numerical comparison. Nat Hum Behav 1:1–8 Available at: https://www.nature.com/articles/s41562-017-0145 [Accessed November 13, 2023].

Stefanac NR, Zhou SH, Spencer-Smith MM, O'Connell R, Bellgrove MA (2021) A neural index of inefficient evidence accumulation in dyslexia underlying slow perceptual decision making. Cortex 142:122–137 Available at: https://research.monash.edu/en/publications/a-neural-index-of-inefficient-evidence-accumulation-in-dyslexia-u [Accessed July 20, 2023].

Steinemann NA, O'Connell RG, Kelly SP (2018a) Decisions are expedited through multiple neural adjustments spanning the sensorimotor hierarchy. Nat Commun 9 Available at: /pmc/articles/PMC6128824/ [Accessed November 13, 2023].

Steinemann NA, O'Connell RG, Kelly SP (2018b) Decisions are expedited through multiple neural adjustments spanning the sensorimotor hierarchy. Nat Commun 9 Available at: /pmc/articles/PMC6128824/ [Accessed November 13, 2023].

Sun JH, Tan L, Yu JT (2014) Post-stroke cognitive impairment: epidemiology, mechanisms and management. Ann Transl Med 2:80 Available at: https://pmc.ncbi.nlm.nih.gov/articles/PMC4200648/ [Accessed March 5, 2025].

Tachibana H, Toda K, Aragane K, Sugita M (1993) Chronometrical analysis of event-related potentials and reaction time in patients with multiple lacunar infarcts. Cognitive Brain Research 1:193–196.

Tagliabue CF, Veniero D, Benwell CSY, Cecere R, Savazzi S, Thut G (2019) The EEG signature of sensory evidence accumulation during decision formation closely tracks

subjective perceptual experience. Scientific Reports 2019 9:1 9:1–12 Available at: https://www.nature.com/articles/s41598-019-41024-4 [Accessed September 22, 2024].

Twomey DM, Kelly SP, O'Connell RG (2016) Abstract and Effector-Selective Decision Signals Exhibit Qualitatively Distinct Dynamics before Delayed Perceptual Reports. The Journal of neuroscience 36:7346–7352 Available at: https://pubmed.ncbi.nlm.nih.gov/27413146/ [Accessed November 13, 2023].

Twomey DM, Murphy PR, Kelly SP, O'Connell RG (2015) The classic P300 encodes a build-to-threshold decision variable. Eur J Neurosci 42:1636–1643 Available at: https://pubmed.ncbi.nlm.nih.gov/25925534/ [Accessed June 26, 2023].

Ulrichsen KM, Alnæs D, Kolskår KK, Richard G, Sanders AM, Dørum ES, Ihle-Hansen H, Pedersen ML, Tornås S, Nordvik JE, Westlye LT (2020) Dissecting the cognitive phenotype of post-stroke fatigue using computerized assessment and computational modeling of sustained attention. European Journal of Neuroscience 52:3828–3845 Available at: https://onlinelibrary.wiley.com/doi/full/10.1111/ejn.14861 [Accessed June 27, 2023].

Van Kempen J, Loughnane GM, Newman DP, Kelly SP, Thiele A, O'Connell RG, Bellgrove MA (2019) Behavioural and neural signatures of perceptual decision-making are modulated by pupil-linked arousal. Elife 8.

Van Kessel ME, Van Nes IJW, Geurts ACH, Brouwer WH, Fasotti L (2013) Visuospatial asymmetry in dual-task performance after subacute stroke. J Neuropsychol 7:72–90 Available at: https://pubmed.ncbi.nlm.nih.gov/23126258/ [Accessed September 26, 2023].

van Vugt MK, Beulen MA, Taatgen NA (2019a) Relation between centro-parietal positivity and diffusion model parameters in both perceptual and memory-based decision making. Brain Res 1715:1–12.

van Vugt MK, Beulen MA, Taatgen NA (2019b) Relation between centro-parietal positivity and diffusion model parameters in both perceptual and memory-based decision making. Brain Res 1715:1–12.

von Lautz A, Herding J, Blankenburg F (2019) Neuronal signatures of a random-dot motion comparison task. Neuroimage 193:57–66.

Wechsler D (2008) Wechsler Adult Intelligence Scale, Fourth Edition (WAIS-IV)

Woodman GF, Luck SJ (1999) Electrophysiological measurement of rapid shifts of attention during visual search. Nature 400:867–869.

Wyart V, de Gardelle V, Scholl J, Summerfield C (2012) Rhythmic fluctuations in evidence accumulation during decision making in the human brain. Neuron 76:847–858 Available at: https://pubmed.ncbi.nlm.nih.gov/23177968/ [Accessed September 22, 2024].

Xi G, Keep RF, Hoff JT (2006) Mechanisms of brain injury after intracerebral haemorrhage. Lancet Neurol 5:53–63.

Yartsev MM, Hanks TD, Yoon AM, Brody CD (2018) Causal contribution and dynamical encoding in the striatum during evidence accumulation. Elife 7.

Zhou Y, Freedman DJ (2019) Posterior parietal cortex plays a causal role in perceptual and categorical decisions. Science 365:180–185 Available at: https://pubmed.ncbi.nlm.nih.gov/31296771/ [Accessed September 22, 2024].

Figures and figure legends

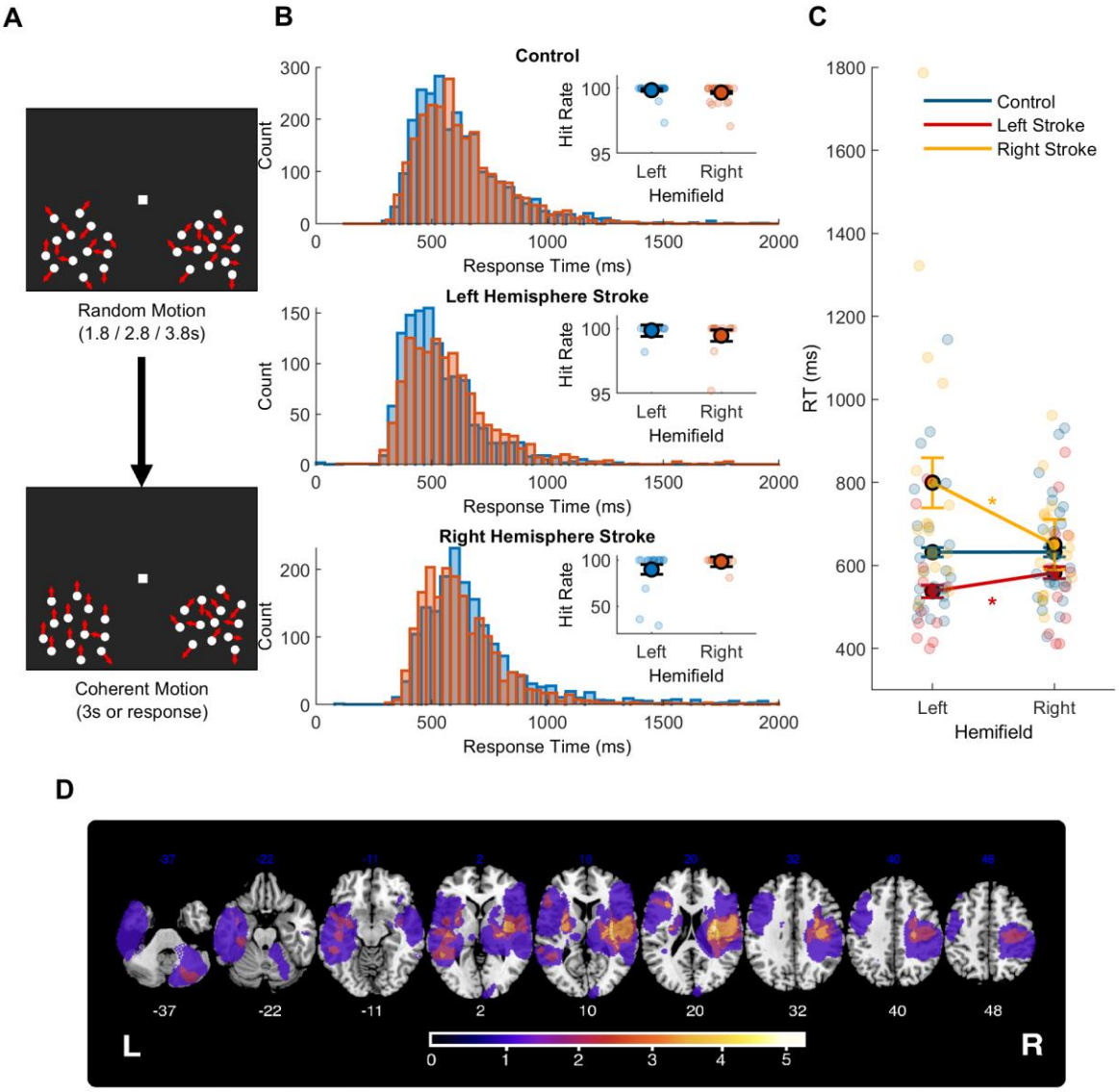

Figure 1 Perceptual Decision-Making Task Reveals Slowed Contralesional Responding Post-Stroke. (**A**) Schematic of the BRDM task. Beginning with central fixation, each dot moved randomly at a rate of 5 degrees per second. Following a period of random motion lasting either 1.8, 2.8, or 3.8 seconds, 90% of the dots in one patch began moving uniformly, either up or down. Participants were 1 to respond to these coherent motion targets with a single mouse click with their right index finger (left index finger for *n*=2 patients with right-sided hemiplegia). (**B**) Performance on the BRDM task, with trials in which target motion was presented in the left or right hemifield plotted separately. Histograms depict the response time

for each valid trial (i.e., where central fixation was maintained, there were no artefacts in the EEG/eye-tracking data, and a response was made between 150ms post-stimulus onset and stimulus offset) across all participants within a given group. Note that responses up to 3000ms were permitted, but for clarity only responses up to 2000ms are visualised here. Mean hit rate for each participant is depicted via inset scatterplots. (**C**) Mean reaction time for left and right hemifield target trials for each group, with individual participant means plotted as single points. (**D**) Lesions overlaid for n=21 patients with available clinical neuroimaging (n=11 left hemisphere, n=10 right hemisphere). Voxel colour indicates the number of overlapping lesions present at each region (range = 1-4). Lesions are coloured according to the number of overlapping voxels between participants. Individual lesion masks, network disconnection summaries, and cortical integrity statistics can be found in Figures S1 and S2, and Table S3, respectively. Significant (p<.05) within-group differences are denoted by asterisks. Within-subject error bars are depicted.

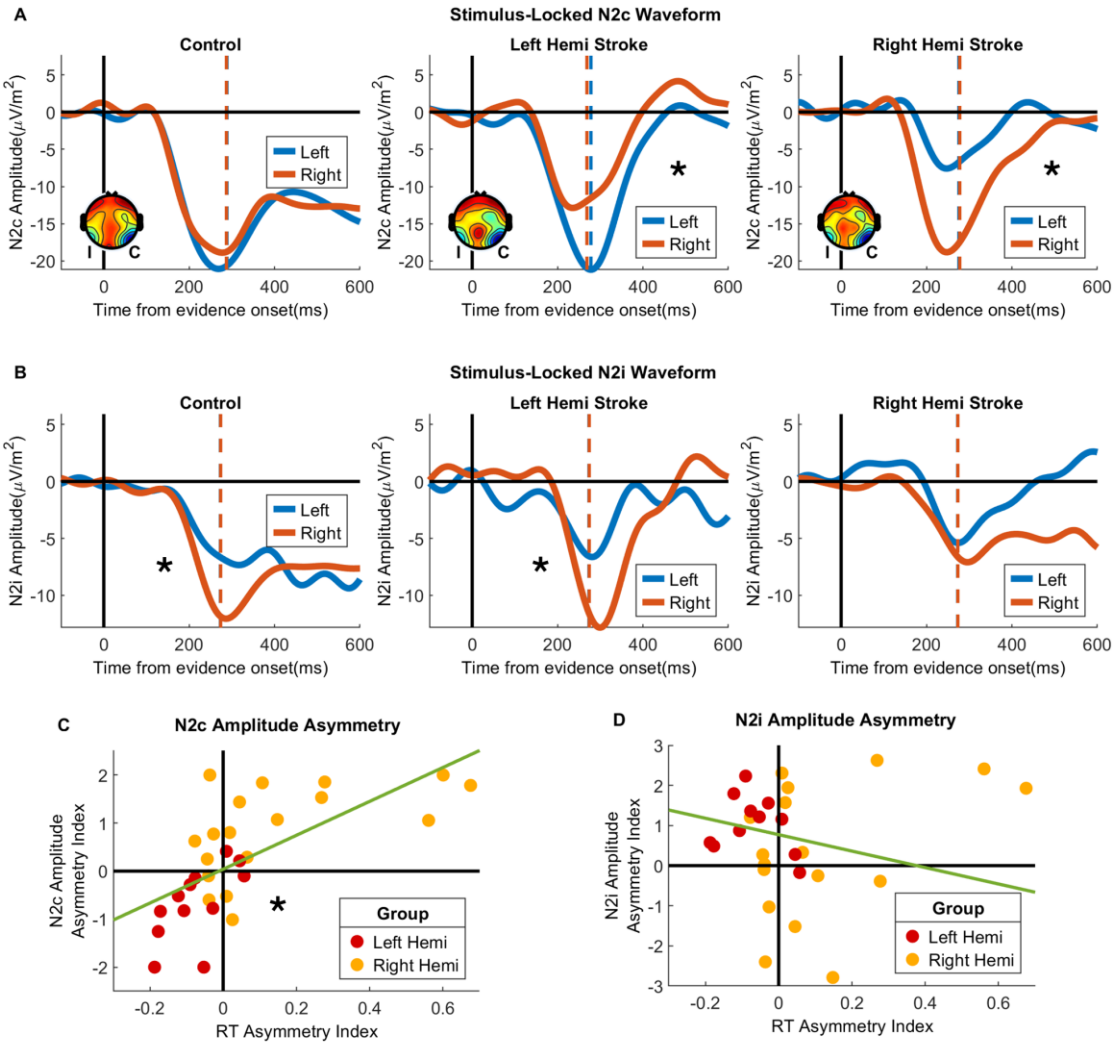

Figure 2 Reduced N2c, but not N2i, Amplitude in the Stroke-Affected Hemisphere Indexes Slowed Responding to Contralesional Space. (**A**) N2c waveforms extracted from temporal electrodes contralateral to target hemifield (T7 and T8 for right and left hemifield targets, respectively). Inset topoplots show average scalp electrical activity during 250-280ms windows post-stimulus onset for each group separately. Note that 'I' and 'C' denote ipsilateral and contralateral signals (such that ipsilateral shows the grand average of left hemisphere activity for left hemifield targets, and right hemisphere activity for right hemifield targets, and vice versa). (**B**) N2i waveforms extracted from temporal electrodes ipsilateral to target hemifield (T8 and T7 for right and left hemifield targets, respectively). (**C, D**) The relationship

between RT asymmetry index and N2c amplitude asymmetry index for patients. A least squares regression line is fitted for reference. Significant results are represented by *.

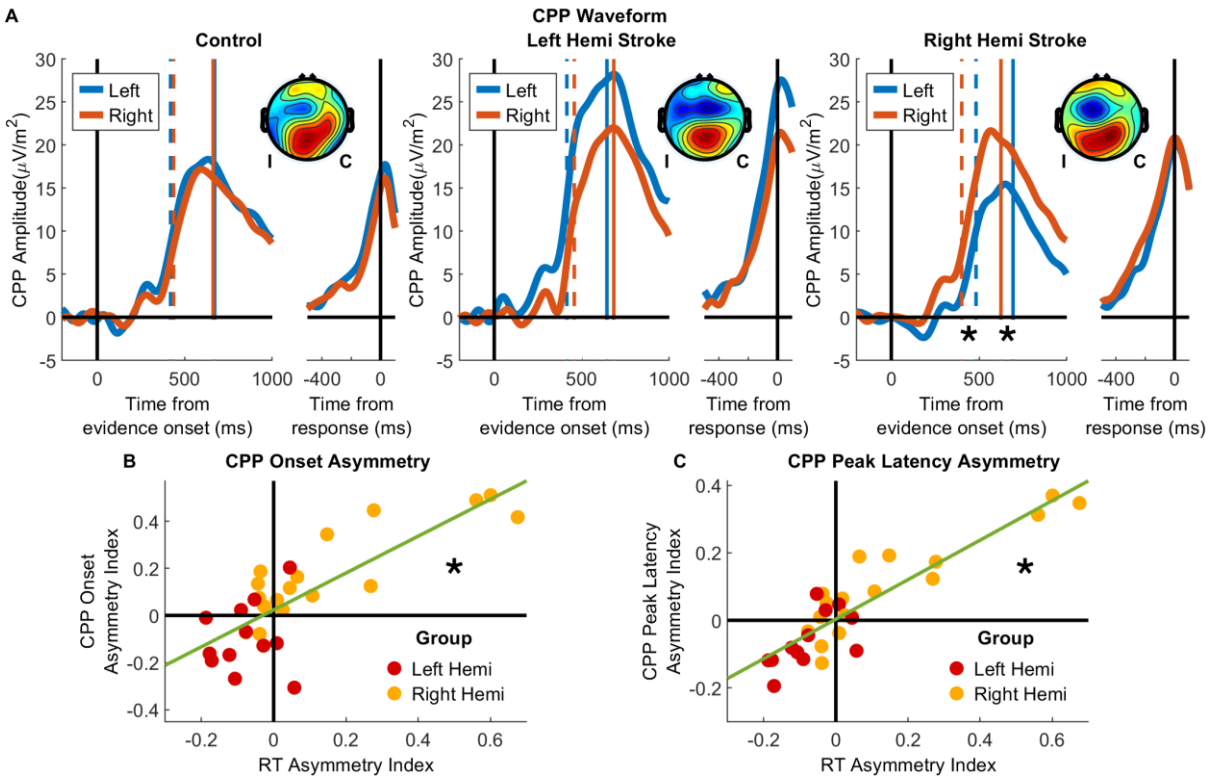

Figure 3 Delayed CPP Onset and Later Peak Latency Index Slowed Contralesional Responding. (**A**) Stimulus- and Response-Locked CPP waveforms extracted from electrode Pz, presented separately for each group and for left and right hemifield targets. Inset topoplots reflect average activity between 600-700ms post-stimulus onset for contra- (C) and ipsilateral (I) targets. Dashed lines signify calculated CPP onset, and solid vertical lines indicate CPP peak latency. (**B**) Relationship between the CPP onset asymmetry index (where more positive values suggest delayed onset for left hemifield targets) and RT asymmetry index (where more positive values suggest slower responding to left hemifield targets). A least squares regression line is fitted for reference. (**C**) Scatter plot of participant means depicting the relationship between CPP peak latency index (where more positive values suggest delayed peaks for left hemifield targets) and RT asymmetry index (where more positive values suggest slower responding to left hemifield stimuli). Significant results are indicated by *.

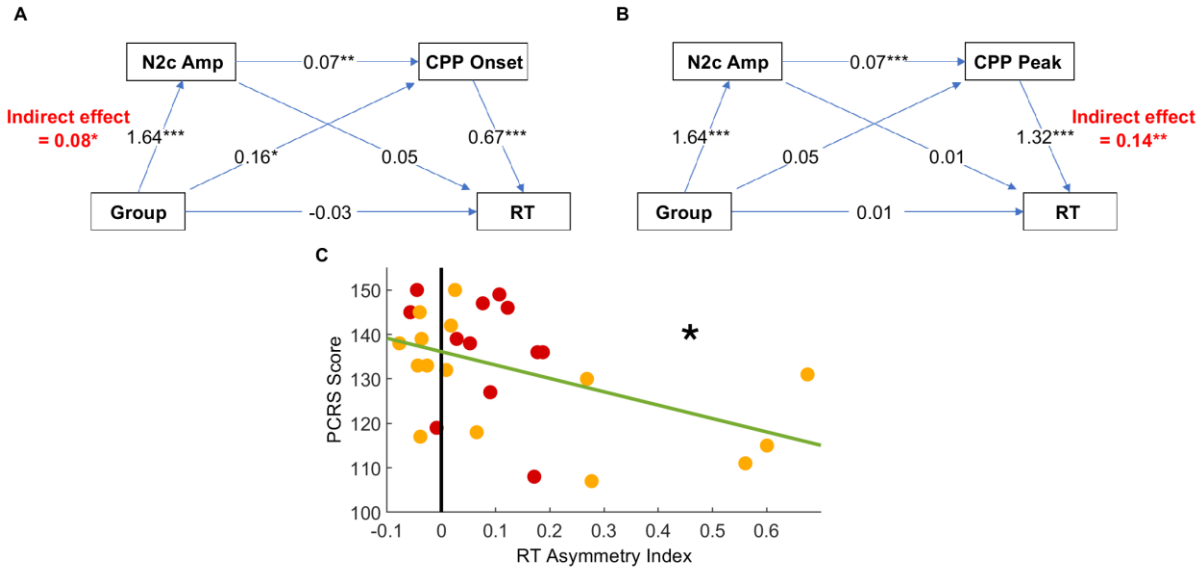

Figure 4 Relationship Between Stroke Side and Contralesional Slowing is Mediated by N2c and CPP Asymmetries. Serial mediation models of lesion side → RT asymmetry including CPP onset latency (**A**) and CPP peak latency (**B**) asymmetries. * p<.05, ** p<.01, *** p<.001. Also depicted is a scatterplot demonstrating the relationship between the self-reported everyday functioning measure (PCRS) and RT asymmetry (**C**).

Tables and table legends

Table 1

Demographic Information Across Groups

	Sex (*n*)		Recruited From (*n*)		Age (Years)	Education (Years)	Premorbid IQ [a]	Cognitive Reserve Index (CRI) [b]
	Male	**Female**	**Australia**	**UK**				
Healthy Controls	13 (48.15%)	14 (51.85%)	27 (100.00%)	0 (0.00%)	73.44 (7.06) 57-90	15.30 (3.69) 10-23	117.35 (5.95)* 106-129	145.32 (18.47)* 115-184
Post-Stroke Patients	16 (53.33%)	14 (46.67%)	11 (36.67%)	19 (63.33%)	70.40 (7.99) 53-84	14.58 (3.86) 3-21	108.96 (11.19) 84-123	127.63 (19.47) 94-182
Left Hemisphere	5 (41.67%)	7 (58.33%)	6 (50.00%)	6 (50.00%)	69.50 (7.62) 58-84	14.46 (3.42) 9-20.5	107.42 (11.80)* 84-121	125.00 (12.17) 100-138
Right Hemisphere	11 (61.11%)	7 (38.89%)	5 (27.78%)	13 (72.22%)	71.00 (8.39) 53-84	14.67 (4.22) 3-21	110.20 (10.92) 89-123	129.73 (24.02) 94-182

Note. Values presented are mean, standard deviation, and range unless stated otherwise. [a] Values estimated using the National Adult Reading Test (NART) according to updated Wechsler Adult Intelligence Scale – Fourth Edition (WAIS-IV) norms. Note that these data were available for *n*=17 controls, *n*=12 left hemisphere, and n=15 right hemisphere patients. [b] As calculated using the Cognitive Reserve Index questionnaire (CRIq). Note that these data were available for *n*=22 controls, *n*=12 left hemisphere, and n=15 right hemisphere patients. * $p<.05$.

Table 2

Stroke Characteristics

	Stroke Hemisphere	
	Left	**Right**
Stroke Mechanism (*n*)		
Ischaemic	8	17
Haemorrhagic	3	1
Transformation [a]	1	0
Stroke Territory (*n*)		
MCA	10	15
PCA	1	3
ACA/MCA	1	0
Years Since Stroke	2.99 (2.14) 0.22-6.54	3.92 (3.22) 0.22-11.91
Stroke Volume (cm^3) [b]	24.10 (40.56) 0.04-113.78	38.30 (40.10) 0.29-116.11
NIHSS (Admission) [c]	5.60 (4.93) 1-13	10.17 (6.49) 4-22
Documented Neglect as Inpatient (*n*) [d]	0 (0.00%)	10 (52.63%)

Note. Values presented are mean, standard deviation, and range unless stated otherwise. [a] Transformation denotes a stroke that was initially ischaemic and developed haemorrhagic features. [b] Estimates provided based on available clinical scans for *n*=11 left and *n*=10 right hemisphere stroke participants (*n*=9 with CT, *n*=12 MRI data; see Imaging Data for further information). [c] National Institutes of Health Stroke Scale score on admission to hospital. Scores

range from 0-42 with lower scores suggestive of a less severe stroke. Note that these data were only available for n=5 left hemisphere and n=6 right hemisphere stroke participants. [d] Participants were considered to have a documented history of spatial neglect if: (1) medical records described symptoms consistent with the syndrome; or (2) performance on a cancellation task as an inpatient was supportive of neglect according to medical records. Note that only n=17 (n=6 left hemisphere stroke, n=11 right hemisphere stroke) had a cancellation task administered acutely. * p<.05.

Table 3

Cognitive Test Data by Group

Test	Left Hemisphere Stroke		Right Hemisphere Stroke	
	Mean (SD)	% Impaired	Mean (SD)	% Impaired [a]
Oxford Cognitive Screen [b]				
Picture Naming (/4)	3.83 (0.39)	0.0	3.60 (0.74)	13.33
Picture Pointing (/3)	3.00 (0.00)	0.0	3.00 (0.00)	0.0
Orientation (/4)	4.00 (0.00)	0.0	4.00 (0.00)	0.0
Sentence Reading (/15)	14.75 (0.62)	8.3	14.71 (1.07)	7.14
Number Writing (/3)	3.00 (0.00)	0.0	2.87 (1.07)	6.67
Calculation (/4)	3.67 (0.65)	8.3	3.67 (0.62)	6.67
Heart Cancellation – Total (/50)	47.00 (2.76)	8.3	45.20 (6.72)	20.0
Hearts: Object Asymmetry [c]	0.00 (0.00)	0.0	0.13 (0.83)	46.67 (26.67 left; 20.00 right inattention)
Hearts: Space Asymmetry [c]	0.17 (1.27)	0.0	0.73 (3.08)	6.67
Imitation (/14)	11.08 (0.79)	0.0	10.27 (2.05)	0.0
Verbal Memory (/4)	3.75 (0.45)	0.0	3.87 (0.35)	0.0
Episodic Recognition (/4)	3.67 (0.49)	0.0	3.93 (0.26)	0.0
Executive – Mixed Task Time (s)	47.5 (58.87)		51.57 (33.45)	
Executive Total Score [d]	-1.00 (2.66)	0.0	-0.47 (3.16)	6.67
Auditory Attention Task				
Total Score (/54)	51.58 (5.12)		51.40 (4.94)	
False Positives (/27)	0.92 (1.98)		1.33 (2.58)	

Omissions (/27)	1.25 (2.73)	1.33 (2.66)
Sustained Attention Index (-18 to +18) [e]	-0.08 (0.67)	0.07 (0.96)
Landmark Task [f]	0.15 (0.27)	0.10 (0.25)
Patient Competency Rating Scale (/150)	136.67 (12.89)	129.40 (12.98)

Note. [a] Proportions for the OCS are reported for the *n*=15 right hemisphere participants that completed this task. *n*=1 of these participants did not complete the Sentence Reading subtest. [b] Impairment cutoffs as per (Demeyere et al., 2015). [c] Asymmetry scores are calculated such that scores > 0 denote spatial bias toward the right, whereas scores < 0 reflect bias toward the left. [d] Executive score denotes the difference in accuracy between simple and complex speeded tasks, whereby higher scores reflect relatively poorer performance on more complex tasks. [e]Sustained Attention Index compares performance on the first and last blocks, such that higher scores denote poorer performance on later trials. [f] *n*=1 left hemisphere participant did not complete this task.